

Cite this: *Soft Matter*, 2011, **7**, 2352

www.rsc.org/softmatter

Lane formation in driven mixtures of oppositely charged colloids†

Teun Vissers,^{*a} Adam Wysocki,^{‡b} Martin Rex,^b Hartmut Löwen,^b C. Patrick Royall,^{§a} Arnout Imhof^a and Alfons van Blaaderen^a

Received 18th November 2010, Accepted 22nd December 2010

DOI: 10.1039/c0sm01343a

We present quantitative experimental data on colloidal laning at the single-particle level. Our results demonstrate a continuous increase in the fraction of particles in a lane for the case where oppositely charged particles are driven by an electric field. This behavior is accurately captured by Brownian dynamics simulations. By studying the fluctuations parallel and perpendicular to the field we identify the mechanism that underlies the formation of lanes.

Far from thermodynamic equilibrium, a wealth of fascinating self-organization processes can emerge along with unusual pattern formation and novel transport properties.^{1,2} One of the simplest prototypes of non-equilibrium pattern formation is lane formation, exhibited by dusty plasmas,^{3,4} granular matter,⁵ pedestrian dynamics,^{6,7} and army ants.⁸ In this paper, we characterize the patterning and dynamical signatures of lane formation in a colloidal system experimentally and with computer simulations. Our results may find use in electronic ink, which also contains oppositely charged colloids that are driven by electric fields.^{9,10}

A fundamental and microscopic understanding of non-equilibrium phenomena requires resolving the underlying dynamical processes on the scale of the individual particles. For this, colloidal dispersions are excellent model systems since they can be brought out of equilibrium in a controlled way by external fields and the trajectories of the individual particles can be tracked in real space using confocal microscopy, which allows unparalleled comparison with computer simulation and particle-level theory.^{11–13} Here, we first study the formation of lanes in driven colloidal mixtures as a function of the driving strength using both experiments and Brownian dynamics computer simulations. Lane formation in this 3D system is found to be a continuous process as a function of driving field. Starting from an initial mixed state, the dynamical mechanism behind the formation of lanes is identified: there is an enhanced lateral mobility of particles induced by collisions with

particles driven in the opposite direction, which sharply decreases once lanes are formed. Therefore, particles in a lane can be regarded as being in a dynamically ‘locked-in’ state.

In our experiments, we used a binary dispersion of sterically stabilized, nearly equal sized, but oppositely charged polymethylmethacrylate (PMMA) spheres inside a rectangular capillary. The particles were synthesized by dispersion polymerization,¹⁴ and fluorescently labeled with either 7-nitrobenzo-2-oxa-1,3-diazole (NBD) or rhodamine isothiocyanate (RITC). The two species are color-coded as ‘green’ ($\sigma_{\text{green}} = 1.06 \mu\text{m}$, polydispersity 6%, NBD-labeled) and ‘red’ ($\sigma_{\text{red}} = 0.91 \mu\text{m}$, polydispersity 7%, RITC-labeled). The overall volume fraction of the suspension $\phi_{\text{green}} (0.090) + \phi_{\text{red}} (0.090)$ was 0.18.

To match the density and refractive index of the particles with the solvent, the particles were dispersed in a mixture of 27.2 w% *cis*-decahydronaphthalene and cyclohexylbromide containing 75 μM tetrabutylammonium bromide. From the conductivity of the salt-containing solvent (4.9 nS cm^{-1}), we estimated the solvent micro-ion concentration to result in a Debye–Hückel screening length of $\kappa^{-1} \approx 170 \text{ nm}$. This dispersion was transferred to a capillary cell (Vitrocom, Fig. 1a) with two 50 μm (diameter) nickel alloy wires (Goodfellow) threaded along the length direction (y , horizontal) and closed with either UV-glue (Norland) or wax. Experimental data obtained by confocal laser scanning microscopy (Leica, SP2) is presented from an optical slice with thickness $\Delta z \approx 2 \mu\text{m}$. We used a tracking algorithm to obtain the particle coordinates for each confocal image and track their trajectories in time. The coordinates of each species were determined and then the mean displacement between consecutive frames was obtained *via* cross-correlation of the coordinates similar to Ref. 15. This mean displacement was then subtracted to track each particle in time. Red and green species were treated separately.

In the case of zero field $E = 0$, the oppositely charged colloids eventually crystallized. However, this occurred on a time scale of days,^{13,16} and thus is not relevant to laning. For $|E| > 0$, opposite motion of two colloidal species was induced and lane-like structures formed in the field direction. In the experiments, electro-osmosis on the capillary glass walls leads to a fluid-flow profile across the cell in the z -direction.¹⁷ We determined the lower theoretical stationary layer (or plane of zero-velocity), where the macroscopic fluid flows resulting from electro-osmosis cancel each other, to be at $z_{\text{stat}} \approx 26 \mu\text{m}$ from the lower wall (Supplementary Fig. 2).

We use Brownian dynamics simulations for the colloidal particles which interact *via* a screened Coulomb (or Yukawa) pair

^aSoft Condensed Matter, Debye Institute for Nanomaterials Science, Utrecht University, Princetonplein 5, 3584 CC Utrecht, The Netherlands. E-mail: t.vissers@uu.nl; a.vanblaaderen@uu.nl

^bInstitut für Theoretische Physik II, Heinrich-Heine-Universität Düsseldorf, Universitätsstrasse 1, D-40225 Düsseldorf, Germany

† Electronic supplementary information (ESI) available. See DOI: 10.1039/c0sm01343a

‡ Current address: Institut für Festkörperforschung, Forschungszentrum Jülich, D-52425 Jülich, Germany.

§ Current address: School of Chemistry, University of Bristol, Bristol, BS8 1TS, UK.

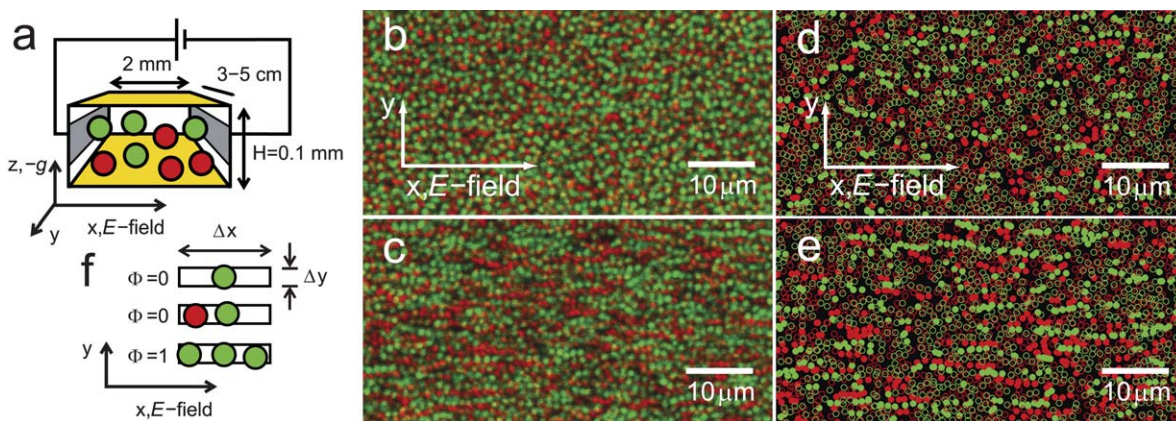


Fig. 1 Lane formation in the experiments and simulations. (a) A sketch of the experimental setup. A suspension of oppositely charged colloidal particles is confined in a millimetre-sized capillary. Green are negatively charged NBD-labeled particles, red are positively charged RITC-labeled particles. The electric field E is directed along the x -axis. (b–e) Snapshots of oppositely charged particles for two different electric driving fields $E = 30 \text{ kV m}^{-1}$ and $E = 110 \text{ kV m}^{-1}$ in our experiments a few seconds after the field was turned on (b,c) and simulations (d,e). In (d,e) particles i with $\Phi_i = 1$ are depicted with filled circles and $\Phi_i = 0$ with open circles. (f) Definition of the lane order parameter Φ . The lane order parameter for particle i is $\Phi_i = 1$ if and only if its neighbors located inside a box of dimensions $\Delta x \times \Delta y$ are of the same species.

potential $V(r_{ij}) = \frac{Z_i Z_j \lambda_B}{(1 + \kappa \bar{\sigma}/2)^2} \frac{e^{-\kappa(r_{ij} - \bar{\sigma})}}{r_{ij}}$, where $r_{ij} = |\mathbf{r}_i - \mathbf{r}_j|$ is the

inter-particle distance, $\lambda_B = \frac{e^2}{4\pi\epsilon_m\epsilon_0 k_B T}$ is the Bjerrum length, Z_i is the particle charge number, ϵ_m is the relative dielectric constant of the medium, ϵ_0 is the dielectric constant of vacuum, k_B is Boltzmann's constant, and T is the temperature. The colloids move in a highly viscous background solvent so that their dynamics are overdamped (*i.e.* inertia is irrelevant). The hard core is approximated by a steep soft sphere potential $V(r) = V_0(\bar{\sigma}/r)^{24}$, where $V_0 = |V_{r,g}(\bar{\sigma})|$ is the Yukawa interaction strength between red and green particles at distance $\bar{\sigma}$. For simplicity $\bar{\sigma}$ is set to $0.93 \mu\text{m}$ for both species.¹⁸

The electric field $\mathbf{E} = E\mathbf{e}_x$ in the x -direction yields an external driving force. In the so-called Hückel limit, *i.e.* at low salt concentration such that $\kappa\bar{\sigma} \ll 1$, the electrophoretic drift velocity is $v = ZeE/(3\pi\eta\bar{\sigma})$, where η is the solvent viscosity. Since in our case $\kappa\bar{\sigma} \approx 6.0$, we apply a scaled external force to match the electrophoretic drift velocity at finite $\kappa\bar{\sigma}$. The force on the i th particle caused by the applied electric field \mathbf{E} reads $\mathbf{f}_i = Ze\mathbf{E}f(\kappa\bar{\sigma})/(1 + \kappa\bar{\sigma}/2)$, where $f(\kappa\bar{\sigma})$ is the Henry function which is close to unity (1.1) for our parameters.¹⁹ To obtain the trajectories of the colloids we integrate the equation of motion numerically²⁰ with a time-step $\Delta t = 0.0001\tau_D$, where $\tau_D = \bar{\sigma}^2/4D_0$ is the time a particle needs to diffuse its own diameter and $D_0 = k_B T/(3\pi\eta\bar{\sigma})$. Hydrodynamic interactions (HI) between the particles are neglected which we argue is reasonable at moderate volume fractions in electric driving fields since in electrophoresis the opposing motion of the micro-ions with respect to the colloids leads to screening of the HI.²¹ Inclusion of HI at the Long-Ajdari level has negligible impact on laning phenomena for *oppositely charged colloids*.²² A quiescent (*i.e.* flow-free) solvent is assumed to match the zero-velocity observation plane selected in the experiment. The Brownian dynamics computer simulations were performed in 3D in a rectangular box with periodic boundary conditions in all three directions. The colloid volume fraction ϕ (Supplementary Fig. 1), composition of the binary mixture, $\eta = 2.72 \text{ cP}$, solvent dielectric constant $\epsilon_m = 5.6$, Bjerrum length $\lambda_B = 10.0 \text{ nm}$ and screening length $1/\kappa$ are taken to be similar to the experiments. From electrophoresis

experiments and comparing our Brownian dynamics computer simulations with laning experiments, we estimate the particle charges $Ze = -42e$ for the green particles and $Ze = 67e$ for the red particles. More details can be found in the supplementary information.

Typical particle configurations in the steady state at low and high driving fields are shown in Fig. 1 both from experiments (Fig. 1b,c) and from computer simulations (Fig. 1d,e); see also Supplementary Videos 1 and 2 for experimental data recorded at low and high field strength respectively. The simulation shows particles in a thin slice corresponding to the diffraction limited optical section in the experiments. At high driving fields (Fig. 1c,e), the formation of lanes (or strings) of equally charged particles is visible along the field direction in the experiments and simulations.

To quantify the degree of laning, we introduce an order parameter Φ which is defined as follows (see also Fig. 1f). Particles within a thin slice (x,y ; $\Delta z = 2 \mu\text{m}$) are projected on the (xy) -plane. In this plane, a rectangle of length $\Delta x = 3\bar{\sigma}$ along the driving field and width $\Delta y = \bar{\sigma}$ perpendicular to it is constructed around each particle i . We define $\Phi_i = 1$ when all the particles contained in this rectangle are of the same species as particle i . When there are one or more particles of the other species present, $\Phi_i = 0$. In the rare case that only particle i itself is present in the rectangle, $\Phi_i = 0$. The laning order parameter $\Phi = \frac{1}{N} \sum_{i=1}^N \Phi_i$ is now averaged and thus represents the fraction of particles that are in a lane-like environment. Note that Φ has a non-zero value even when no E -field is applied since in the fluid state there are always some particles aligned with the field axis by chance. Therefore Φ should be compared to its zero-field reference value and only the excess of Φ is an indication for laning.

To study the degree of laning in the system as a function of the field strength, we gradually increased and decreased the applied electric field (between -110 V mm^{-1} and 110 V mm^{-1} , Supplementary Video 3) as a function of time t according to a triangular function (Fig. 2a). The rise and fall of Φ is completely symmetric within the accuracy in this field strength domain, with no detectable hysteresis. We also observed no de-mixing; after the field was switched off, we always regained the initial mixed state. In all cases, Φ increased

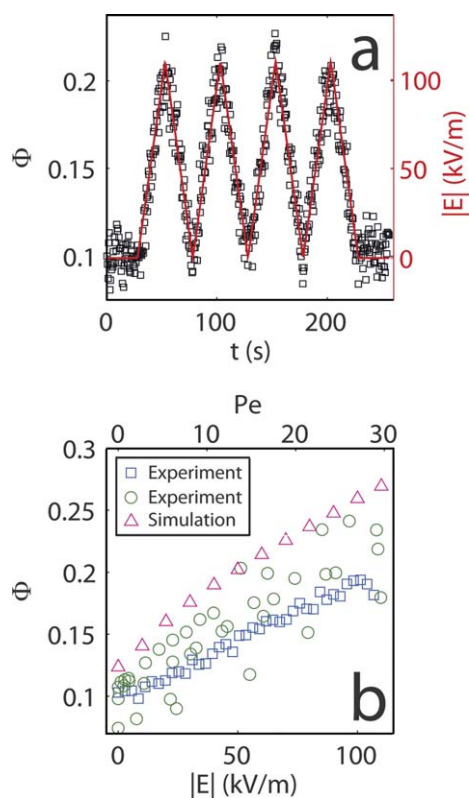


Fig. 2 Lane order as function of field strength. (a) The time evolution of Φ with the gradually increasing and decreasing field in the experiments. The red line depicts the rise and fall of the electric field strength. Squares are experimental data. (b) The order parameter Φ as a function of the electric field strength $|E|$ for experiments in which the field was gradually changed (blue \square) or applied instantaneously (green \circ) and for simulations at constant field strength (magenta \triangle).

monotonically with the field strength, *i.e.* the number of particles in a lane-like environment increased continuously with $|E|$. This trend was unaffected by electro-osmosis (Supplementary Fig. 3). We also studied the formation of lanes when the field was switched on instantly (squares and circles in Fig. 2b), and kept for a few seconds at a constant driving strength. There is no notable difference to the previous data which again indicates that the relaxation towards the steady state was complete in both cases. The degree of laning obtained from the computer simulations (triangles in Fig. 2b) is in agreement with the experimental data. In conclusion, the laning behavior found here in the considered range of the electric driving field is a continuous process without notable hysteresis. This is different from gravity-driven systems whose hydrodynamic interactions are long ranged.²²

We now consider the dynamical mechanism of lane formation starting from an initial mixed state in more detail. The dynamics are characterized by the electrophoretic mobility $\mu = v/E$, defined as the ratio of the (averaged) drift velocity v to the electric field strength E and the fluctuations perpendicular and parallel to the field axis. The degree of anisotropic fluctuation is embodied in the apparent diffusion coefficients D_{\parallel} and D_{\perp} , parallel and perpendicular to the driving field E , which measure the mean-square particle displacements during a characteristic time interval Δt . In detail, two-dimensional trajectories of the i th particle $\mathbf{r}_i(t) = (r_i^{\parallel}(t), r_i^{\perp}(t))$ are recorded in the observation plane during a time interval Δt and the averages over the

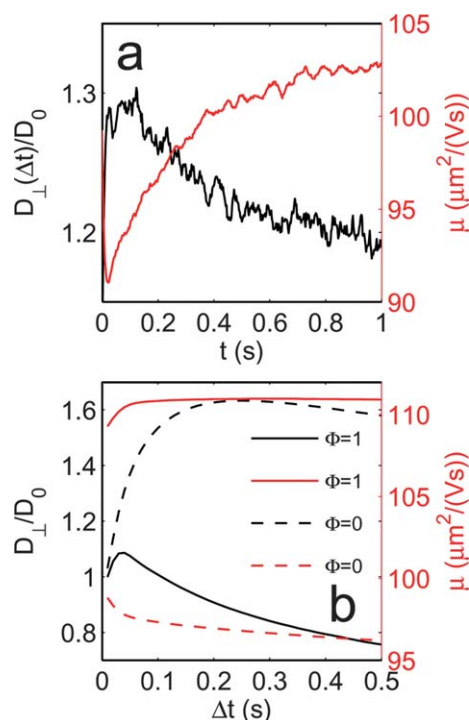


Fig. 3 (a) Time-evolution of diffusivity in the simulations. Apparent perpendicular diffusion coefficient and electrophoretic mobility after application of an electric field of $E = 120 \text{ kV m}^{-1}$ at $t = 0$. (b) Apparent perpendicular diffusion coefficient and electrophoretic mobilities in the simulations after reaching the steady state. We differentiated between lane and non-lane particles, *i.e.* particles have either $\Phi_i = 1$ or $\Phi_i = 0$ over the whole time interval considered. In this case we used a 3D (cylindrical, radius $r = 0.5\sigma$, length $\Delta x = 3\sigma$) order parameter box instead of the 2D rectangular box used in Fig. 2. The data in (a,b) are shown for the red particles, data for the green particles showed the same trend. In (a), the time-interval over which the apparent diffusion coefficient was obtained is $\Delta t = 0.025 \text{ s}$.

particles are calculated $D_{\alpha}(t, \Delta t) = \langle (\Delta r_{\alpha}^i(t, \Delta t) - \langle \Delta r_{\alpha}^i(t, \Delta t) \rangle)^2 \rangle / (2\Delta t)$ with $\Delta r_{\alpha}^i(t, \Delta t) = r_{\alpha}^i(t + \Delta t) - r_{\alpha}^i(t)$ for $\alpha \in \{\parallel, \perp\}$. The apparent diffusion coefficients are given in units of their infinite dilution counterpart D_0 .

Fig. 3a shows the apparent perpendicular diffusion coefficient and the electrophoretic mobilities during the formation of lanes just after the field has been applied. A sudden increase of the lateral diffusivity emerges which then decays, and *vice versa* for the mobility. The fall in μ and the increase in fluctuations perpendicular to the field are associated with an increase in collisions between oppositely driven particles, which gradually reduces upon lane formation. After approximately 1 s, a steady state was reached. Consequently, particles are highly mobile perpendicular to the drive until they meet neighboring particles of the same species in front of them that shield collisions with incoming particles of the other species. Concomitantly, the lateral fluctuations decrease strongly once the particles are in a lane, explaining lane formation as a dynamical 'lock-in' mechanism.²⁴

Turning to steady-state behavior, in Fig. 3b we consider lateral diffusion and mobility of lane particles ($\Phi_i = 1$) and non-lane particles ($\Phi_i = 0$). In a homogeneous liquid, one expects that diffusion and mobility are isotropic quantities. In the steady state of our driven system, this is far from the case. This dynamical heterogeneity is

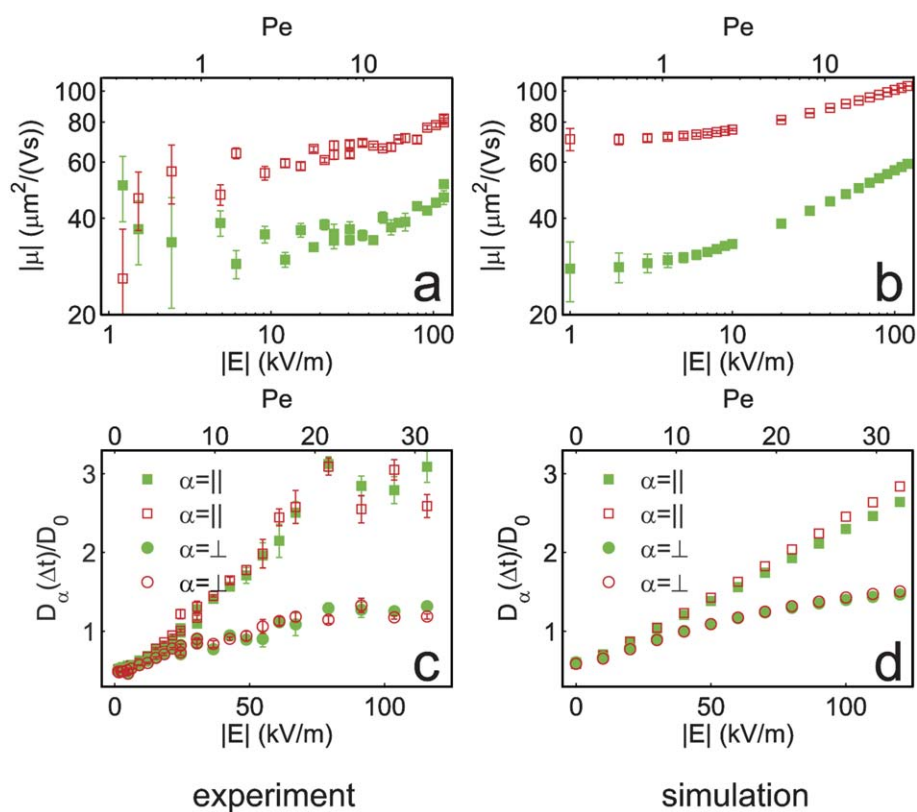


Fig. 4 Field dependence of mobility and diffusivity in the steady state. (a) Electrophoretic mobilities μ from experiments (measured near the lower stationary layer) and (b) simulations as a function of the applied electric field strength $|E|$ for both particle species (red and green colors). The normalized apparent diffusion coefficient D_α/D_0 perpendicular ($\alpha = \perp$) or parallel ($\alpha = \parallel$) to E (with D_0 denoting the short-time diffusion constant at infinite dilution) is shown for (c) experiments and (d) simulations. The time-interval over which the apparent diffusion coefficient was obtained is $\Delta t = 0.5$ s.

coupled to the structural inhomogeneity of laning. Our first observation is that for lane particles, over short measurement times, diffusivity is enhanced due to collisions with particles in other lanes. However, over longer time intervals, because it is confined to a lane, diffusivity is suppressed. Non-lane particles ($\Phi_i = 0$) experience no such confinement: collisions increase the diffusivity up to a plateau value of about $1.6D_0$. Particles in lanes experience relatively few collisions, leading to an enhancement in their mobility, while non-lane particles are constantly buffeted by the oppositely driven particles, leading to a suppression in mobility. These effects could be exploited to steer the transport properties by an external electric field, for example in electronic ink displays or electrophoresis in microfluidics.^{9,10,25}

Finally, we study the driving-field dependence of the anisotropic particle mobility and diffusivity in the steady state. The electrophoretic mobility is shown in Fig. 4a,b. The ratio between driven and diffusive transport measured by Péclet number $Pe = |\mathbf{f}| \sigma / 2k_B T$, where $|\mathbf{f}|$ is the driving force, is also given. The rise of μ with field strength shows a transient scaling regime for intermediate field strengths. There is good agreement between experiment (Fig. 4a) and simulation (Fig. 4b).

Clearly the particle velocity perpendicular to the driving direction is zero but there are non-vanishing fluctuations in the particle displacements. In Fig. 4c,d, D_\perp and D_\parallel are given in the steady state both for experiment and simulation as a function of field strength E . The fluctuations increase in both directions with the electric field but are significantly larger in the drive direction. Simulation data at even

higher fields show, however, that the fluctuations decrease again, pointing to a situation of separated pure lanes which are sliding past each other only at a relatively small interfacial region (Supplementary Fig. 4). Our results are in qualitative agreement with Ref. 23, where the noise amplitude is used as a control parameter instead of the driving field.

We have demonstrated that for our system of oppositely charged colloids, laning is a continuous process. The transient behavior accompanying lane formation shows a link between transport properties, such as electrophoretic mobility and diffusivity, and the local surrounding of the driven particles. In the steady state, dynamic heterogeneity is found between particles in lane and non-lane local environments. The experiments are in good agreement with the computer simulations without hydrodynamics, indicating that HI are not important to explain the lane formation in our driven system. Finally, we have extracted the key mechanism which is responsible for lane formation as a dynamical lock-in process from a disordered state into a lane state. These insights may find use in applications where particles are driven in opposite directions such as in e-ink and microfluidics.

Acknowledgements

The authors thank Johan C.P. Stiefelhagen for particle synthesis and help with the assembly of the electric cells. We thank Michiel Hermes for useful discussions. Peter Helfferich is acknowledged for technical support. This work was supported by DFG/FOM within SFB TR6.

CPR gratefully acknowledges the Royal Society for financial support and TV acknowledges NWO-CW for financial support.

References

- 1 M. C. Cross and P. C. Hohenberg, *Rev. Mod. Phys.*, 1993, **65**, 851.
- 2 A. S. Mikhailov and K. Showalter, *Phys. Rep.*, 2006, **425**, 79.
- 3 G. E. Morfill, *et al.*, *New J. Phys.*, 2006, **8**, 7.
- 4 K. R. Sütterlin, *et al.*, *Phys. Rev. Lett.*, 2009, **102**, 085003.
- 5 M. P. Ciamarra, A. Coniglio and M. Nicodemi, *J. Phys.: Condens. Matter*, 2005, **17**, S2549.
- 6 D. Helbing and P. Molnár, *Phys. Rev. E: Stat. Phys., Plasmas, Fluids, Relat. Interdiscip. Top.*, 1995, **51**, 4282.
- 7 D. Helbing, L. Buzna, A. Johansson and T. Werner, *Transport. Sci.*, 2005, **39**, 1.
- 8 I. D. Couzin and N. R. Franks, *Proc. R. Soc. London, Ser. B*, 2003, **270**, 139.
- 9 B. Comiskey, J. D. Albert, H. Yoshizawa and J. Jacobson, *Nature*, 1998, **394**, 253.
- 10 G. H. Gelinck, *et al.*, *Nat. Mater.*, 2004, **3**, 106.
- 11 A. van Blaaderen and P. Wiltzius, *Science*, 1995, **270**, 1177.
- 12 W. K. Kegel and A. van Blaaderen, *Science*, 2000, **287**, 290.
- 13 M. E. Leunissen, *et al.*, *Nature*, 2005, **437**, 235.
- 14 G. Bosma, *et al.*, *J. Colloid Interface Sci.*, 2002, **245**, 292.
- 15 R. Besseling, L. Isa, E. R. Weeks and W. C. K. Poon, *Adv. Colloid Interface Sci.*, 2009, **146**, 1–17.
- 16 A. P. Hynninen, M. E. Leunissen, A. van Blaaderen and M. Dijkstra, *Phys. Rev. Lett.*, 2006, **96**, 018303.
- 17 R. J. Hunter, *Zeta potential in colloid science: principles and applications* (Academic Press, London, 1981).
- 18 J. Dzubiella, G. P. Hoffmann and H. Löwen, *Phys. Rev. E: Stat. Phys., Plasmas, Fluids, Relat. Interdiscip. Top.*, 2002, **65**, 021402.
- 19 D. Henry, *Proc. R. Soc. London, Ser. A*, 1931, **133**, 106.
- 20 M. P. Allen and D. J. Tildesley, *Computer simulation of liquids* (Oxford University Press, New York, 1991).
- 21 D. Long and A. Ajdari, *Eur. Phys. J. E: Soft Matter Biol. Phys.*, 2001, **4**, 29.
- 22 M. Rex and H. Löwen, *Eur. Phys. J. E*, 2008, **26**, 143.
- 23 D. Helbing, I. J. Farkas and T. Vicsek, *Phys. Rev. Lett.*, 2000, **84**, 1240.
- 24 We remark that laning is also found in a simple model at zero temperature similar to that proposed in L. Corte, P. M. Chaikin, J. P. Gollub and D. J. Pine, *Nat. Phys.*, 2008, **4**, 420, and manifests itself as an absorbing state with a critical signature similar to conserved directed percolation [S. Lübeck, *Int. J. Mod. Phys. B*, 2004, **18**, 3977] (to be published).
- 25 M. A. Rodriguez and D. W. Armstrong, *J. Chromatogr., B: Anal. Technol. Biomed. Life Sci.*, 2004, **800**, 7.